Surface energy balance of the Taylor Glacier, Antarctica.

Andrew Bliss

1 INTRODUCTION

As humans do more to disturb the natural climate system, it is becoming more important for scientists and policymakers to understand the natural system's inherent variability and what feedbacks may exist that could amplify changes that humans make to the atmosphere, oceans, and land surface. One of the best ways to look at what the climate system is capable of is to look at the record of past climate that is contained in proxy records such as ice cores, sediment cores, and the chemical composition of corals. The best time resolution for the interval from 100,000 years ago to the present is provided by ice cores. The ice of Greenland, Antarctica, and a few other glaciers around the world has provided a telling picture of the variations that are possible. The

glacial-interglacial temperature difference has been inferred to be 15 ^{o}C from isotope and borehole temperature data taken at the Greenland Ice Sheet Project II ice core site [1]. Very rapid climate changes have also been observed, such as the Younger Dryas event, in which temperatures dropped almost to the level of the last glacial period. It is thought that the thermohaline circulation of the North Atlantic Ocean plays a significant role in these changes. The nature of the driving force of the circulation means that it has more than one semi-stable configuration, with different states separated by tipping points. If the climate were to pass one of these tipping points in the present day, the implications in terms of human lives affected and monetary losses would be immense.

An important part of the climate system that we need to understand is the glaciers themselves. One glacier in particular, the Taylor Glacier in Antarctica, has a unique potential for informing the way that we think about how Antarctic glaciers have responded to past climate changes. An ice core was drilled at the source of the glacier, at Taylor Dome, in the mid 1990s, providing a local record of the variations in isotopes of water that can provide information about past temperatures at the glacier and at the water vapor source region. Chemical impurities in the ice can provide information about the source and transport of the water vapor. Atmospheric trace gases, such as methane, trapped in bubbles in the ice can provide other information about the climate. Since the Taylor glacier terminates on land, rather than flowing out into the ocean like many other Antarctic glaciers, we have information about past glacier terminus positions from a series of moraines. Another reason to study the Taylor Glacier is the interesting biology that exists in the "dry" valley below the terminus of the glacier. A Long Term Ecological Research Group has been researching in the valley for a number of years, and they will be interested in the results from our work.

The main goal of the Taylor Glacier project is to write a computer model that describes how the glacier flows. We will use the data we collected from Global Positioning System surveying, radar surveying, ablation stake monitoring, and surface isotope sampling in conjunction with data from the Taylor Dome ice core and from the moraines to tune and check the model. The local climatic temperature affects the ice flow part of the glacier model, since ice viscosity has an exponential dependence on temperature. One component of the glacier model is a mass balance model. For the accumulation part of the mass balance, we will use the accumulation record from the ice core to come up with a reasonable mathematical representation of the spatial and temporal pattern of accumulation on the glacier. The ablation part of the mass balance model will be more complex due to variations in the relevant forcing parameters (such as incoming radiation, temperature,

and wind speed) over short distance scales. To understand the relationship between glacier mass balance and climate and to understand the spatial variability of weather parameters across the glacier a network of Campbell Scientific weather stations was installed on the Taylor Glacier in the austral summer of 2003-4. See the map in figure 1 for the locations of the stations. A modelling effort is also underway, buiding upon the work of previous investigators. The models will allow explanation of the measurements and can offer prediction of the mass balance in climates for which there are no measurements. The remainder of this paper will outline a few of the models that have been used by other investigators and will provide some examples of the data that has been collected from the Taylor Glacier.

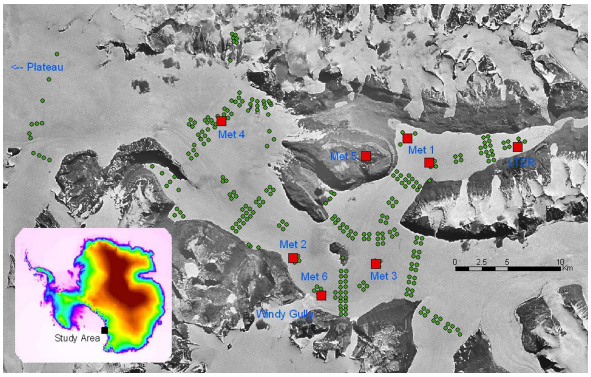

Figure 1: Map of Taylor Glacier, Antarctica. The red squares identify weather station locations. Note that Met 1 moved in early January, so there are two squares for it. The green circles show ablation stake locations. North is up. The inset map is a digital elevation model of Antarctica, showing the general location of the Taylor Glacier.

The simplest measurement to make that is relavent to mass balance is temperature. Models that use just temperature to predict ablation (known as degree day models) have demonstrated remarkable skill for glaciers in temperate climates [2] [3] [4]. Unforunately, in polar climates where the temperature rarely gets above zero degrees Cel-

sius, they do not work very well. Figure 2 shows the temperature for a year on the Taylor Glacier. If one has measurements of tempera-

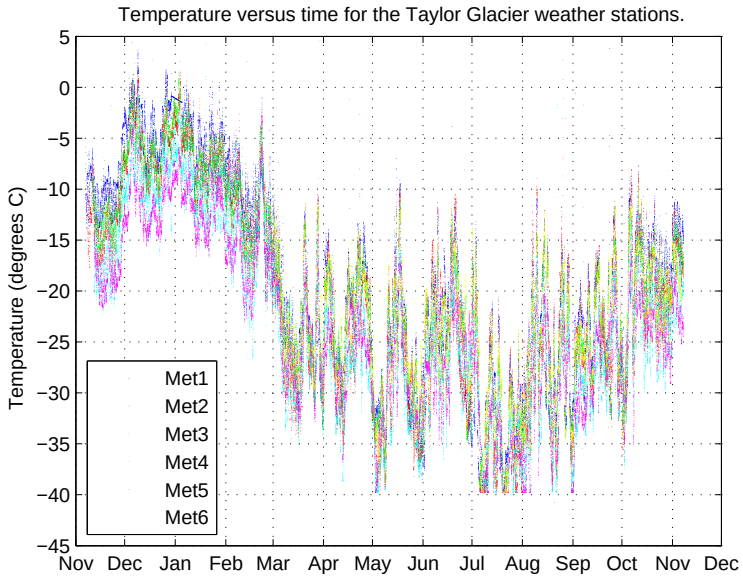

Figure 2: Measured temperature at the six stations we set up on the Taylor Glacier for November 2003 to November 2004. The temperature is rarely greater than zero, rendering most degree-day models ineffective. The legend is somewhat difficult to read: Met1 is blue, Met2 is red, Met3 is green, Met4 is cyan, Met5 is magenta, and Met6 is yellow. The same color scheme is used in all the weather data plots below.

ture, wind speed, and relative humidity along with measurements or assumptions about the radiation budget, one can use an energy balance model (discussed below). Examples of energy-balance models can be found in Strasser *et al.* (Haut Glacier d'Arolla [5]), Brock and Arnold (also Haut Glacier d'Arolla [6]), Reijmer and Oerlemans (Dronning Maud Land [7]), Klok and Oerlemans (Morteratschgletscher [8]), Lewis *et al.* (Canada Glacier [9]), Clow *et al.* (Lake Hoare [10]), and Braithwaite and Olesen (a simple model for sites in Greenland [11]).

A network of weather stations spread over a broad area can help to constrain mesoscale atmospheric models (e.g. [12] [13] [14] [15]), coupled atmosphere and ocean models, and even global climate models [16] [17] [18]. These models include all the physics of energy balance

models, but their complexity (and the corresponding high computer costs) means that their spatial resolution must be significantly lower than that of energy-balance or degree day models. An advantage of the complex models is that they are also capable of predicting accumulation (energy-balance and degree day models can not).

2 THE GENERAL ENERGY-BALANCE EQUATION

The basic equation governing the energy-balance at the surface of a glacier is

$$Q_0 = SW \downarrow (1-\alpha) + LW \downarrow - LW \uparrow + Q_H + Q_L + Q_R \qquad (1)$$

where Q_0 is the flux of energy from the atmosphere to the glacier surface, $SW \downarrow$ is the downwelling (incoming) shortwave radiation, α is the albedo, $LW \downarrow$ is the downwelling longwave radiation, $LW \uparrow$ is the upwelling longwave radiation, Q_H is the sensible heat flux, Q_L is the latent heat flux, and Q_R is the heat flux due to rain falling on the surface. The term $SW \downarrow (1-\alpha)$ could also be written $SW \downarrow - SW \uparrow$ if measurements of both those parameters are available. The flux of energy from the atmosphere to the surface (Q_0) can be used in two ways: to warm a layer of snow or ice near the surface, or to melt snow or ice at the surface. For temperate glaciers where the ice is at the melting point, this flux term can easily be converted to the mass of ice melted: $melt = Q_0/L_f$ where L_f is the latent heat of fusion. The terms in equation 1 which represent changes in the mass balance of the glacier are Q_0 (when ice melt runs off the glacier) and Q_L (evaporation, condensation, and sublimation).

The next five sections will describe the methods and measurements that can be used to determine each of the terms in equation 1. I will then describe the methods that various authors have used to distribute weather station measurements over larger areas of glaciers.

3 SHORTWAVE RADIATION

If measurements of shortwave radiation are available (e.g. figure 3) , they should be used in equation 1 to predict the ablation at the stations.

However, some of the terms in the radiation budget can be predicted without weather station data. For example, incoming shortwave radiation in a cloud free sky can be accurately predicted if one has a digital elevation model for the area. The effect of clouds complicates the

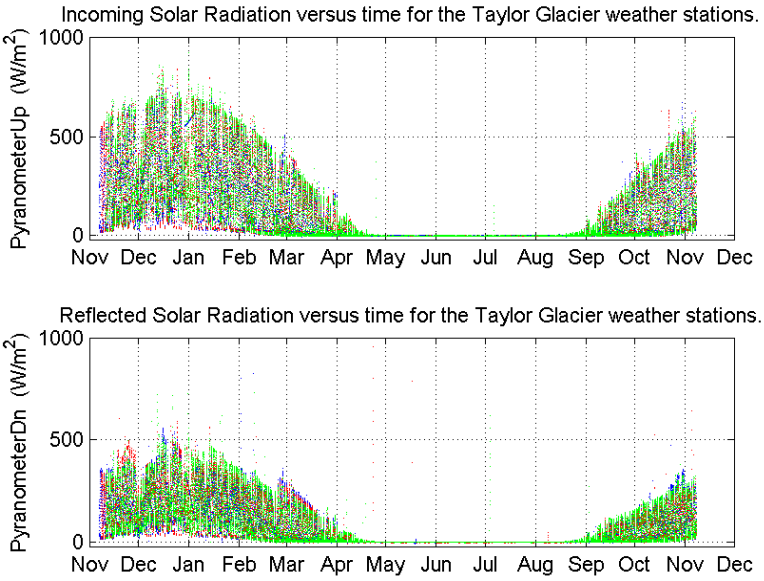

Figure 3: Measured shortwave radiation fluxes for the six stations on the Taylor Glacier. Kipp and Zonen pyranometers were used to measure the radiation.

picture considerably though and parameterizations become necessary. The parameterizations can be tuned at the weather station locations, so that the equations are as accurate as possible for a region, and then used to predict the radiation at points on the glacier away from the weather station.

Greuell and Genthon [19] give one set of equations parameterizing the incoming shortwave radiation. Another, more detailed, outline of the equations comes from Strasser *et al.* [5]. The equations in the two papers are quite similar and in some cases are based on the same earlier references. Below I will describe the equations from Strasser *et al.* [5], with some additional notes based on comparing the paper to the companion computer program AMUNDSEN.

3.1 Direct incoming shortwave radiation

The direct shortwave radiation at a normal incidence angle (I_{direct}) can be parameterized as

$$I_{direct} = 1367\ c\ (\tau_r\ \tau_o\ \tau_g\ \tau_w\ \tau_a + \beta(z)) \tag{2}$$

where 1367 is the top of atmosphere shortwave radiation flux, c is a correction factor for the eccentricity of earth's orbit, τ_r is transmittance due to Rayleigh scattering, τ_o is the transmittance of ozone, τ_g is transmittance by uniformly mixed trace gases, τ_w is the transmittance by water vapor, and τ_a is the transmittance due to aerosols. $\beta(z)$ is an extra correction factor for altitude effects (some of the other parameters already have altitude effects built in). Equations to calculate each of these parameters follow.

$$\begin{aligned} c = 1.000110 + 0.034221\ \cos(\Gamma) + 0.001280\ \sin(\Gamma) \\ +0.000719\ \cos(2\Gamma) + 0.000077\ \sin(2\Gamma) \end{aligned} \tag{3}$$

The day angle (Γ) is defined as $\Gamma = \frac{2\ \pi\ (J-1)}{365}$. J is the day of the year.

$$\tau_R = e^{[-0.0903\ m^{0.84}\ (1+m-m^{1.01})]} \tag{4}$$

where m is the relative optical path length computed with

$$m = \left(\frac{p}{1013.25}\ \frac{1}{\cos(\theta_z) + 0.15\ (93.885 - \theta_z)^{-1.253}} \right) \tag{5}$$

where p is the local pressure, 1013.25 is sea level pressure in hPa, θ_z is the solar zenith angle, and the other constants are taken from Kasten [20]. Ozone transmittance (τ_o) is calculated with assumptions about or measurements of the layer thickness (l) of ozone at the glacier. Ozone measurements have been made from satellites with the Total Ozone Mapping Spectrometer (TOMS). The data is available on the web at http://toms.gsfc.nasa.gov/eptoms/ep.html.

$$\begin{aligned} \tau_o = 1 - 0.161\ l\ m + \frac{1}{(1 + 139.48\ l\ m)^{0.3035}} \\ + 0.02715\ l\ m\ \frac{1}{1 + 0.044\ l\ m + 0.0003(l\ m)^2} \end{aligned} \tag{6}$$

The transmittance by uniformly mixed trace gases is

$$\tau_g = e^{(-0.0127\ m^{0.26})} \tag{7}$$

The transmittance due to water vapor is calculated with the amount of precipitable water in cm (w).

$$\tau_w = 1 - 2.4959\, w\, m\, \frac{1}{(1 + 79.034\, w\, m)^{0.6828} + 6.385\, w\, m)} \tag{8}$$

w is estimated based on the measured vapor pressure of the air (e_a) at the weather station and the measured air temperature (T_a). From Prata [21]:

$$w = 46.5\, \frac{e_a}{T_a} \tag{9}$$

Aerosol transmittance is

$$\tau_a = (0.97 - 1.265\, v^{-0.66})^{m^{0.9}} \tag{10}$$

where v is the prescribed visibility in km. It might be interesting to see if the aerosol product from the TOMS measurements would be useful for calculating this transmittance. Bintanja's [22] correction for elevation given below applies for elevations below 3000 m. For elevations above that, the value at 3000 m is used. It is not entirely clear from Strasser [5] but one needs to multiply this factor by the elevation.

$$\beta(z) = 2.2 \times 10^{-2}\, km^{-1} \tag{11}$$

3.2 Diffuse incoming shortwave radiation

Diffuse shortwave radiation is calculated in a different manner. In the following discussion, I am not sure if transmittance is the appropriate term, but it is the term that Strasser [5] uses. The transmittances for the diffuse radiation are additive rather than multiplicative. The transmittance of scattered direct radiation due to aerosol absorptance is

$$\tau_{aa} = 1 - (1 - \omega_0)\, (1 - m + m^{1.06})\, (1 - \tau_a) \tag{12}$$

where ω_0 is the single scattering albedo, assumed to be 0.9. τ_{aa} then gets plugged into the following equation to get the transmittance due to Rayleigh scattering.

$$\tau_{rr} = \frac{0.395\, \cos(\theta_z)\, \tau_o\, \tau_g\, \tau_w\, \tau_{aa}\, (1 - \tau_r)}{(1 - m + m^{1.02})} \tag{13}$$

Note: the AMUNDSEN computer program's implementation of the above equation multiplies by $(1 - m + m^{1.02})$ instead of dividing by it. I'm not sure which is correct. An intermediate calculation is made to determine the irradiance due to the diffuse Rayleigh transmittance

$$i_{rr} = 1367\, c\, \tau_{rr} \tag{14}$$

The ratio of forward scattering to total scattering of shortwave radiation by aerosols is

$$F_c = 0.9067 + 0.1409\,\theta_z - 0.2562\,\theta_z^2. \tag{15}$$

The forward scattering ratio is based on a regression of tabulated values from Robinson [23]. F_c is used to determine the transmittance due to aerosol scattering

$$\tau_{as} = \frac{0.79\,\cos(\theta_z)\,\tau_o\,\tau_g\,\tau_w\,\tau_{aa}\,F_c\,(1-\frac{\tau_a}{\tau_{aa}})}{(1-m+m^{1.02})}. \tag{16}$$

The 0.79 prefactor above is not in Strasser [5] but I think it should be, based on the computer program AMUNDSEN. Another intermediate irradiance calculation is performed for the diffuse radiation due to aerosols

$$i_{as} = 1367\,c\,\tau_{as}. \tag{17}$$

The effect of multiple reflections between the atmosphere and ground depends on the incoming radiation, sky albedo, and an area averaged ground albedo

$$i_{mr} = (I_{direct} + i_{rr} + i_{as})\,\frac{a_g\,a_a}{1-a_g\,a_a} \tag{18}$$

where a_a, the atmospheric albedo, is

$$a_a = 0.0685 + (1-F_c)\,(1-\frac{\tau_a}{\tau_{aa}}). \tag{19}$$

For the ground albedo (a_g), Strasser [5] used an average over the whole DEM of the Haut Glacier d'Arolla, an area of about 20 square km. The total diffuse radiation is then

$$I_{diffuse} = (i_{rr} + i_{as} + i_{mr}) \times sky\ view\ factor + i_{tr} \tag{20}$$

where the sky view factor is found using Iqbal's [24] unit sphere method and i_{tr} is the radiation reflected off of the surrounding slopes as calculated following Corripio [25].

Finally, the total global radiation is simply calculated as the sum of the direct and diffuse components of the incoming shortwave radiation.

$$I = I_{direct} + I_{diffuse} \tag{21}$$

Even if high-quality measurements of global radiation exist for a particular place, an accurate calculation of the global radiation is important because it is used along with the measurements to calculate cloud factors. Cloud factors, in turn, are important for predicting or extrapolating longwave radiation (see details below). The global radiation is, of course, only half of the shortwave radiation budget equation. The outgoing (reflected) shortwave radiation is the other half.

3.3 Outgoing shortwave radiation

The outgoing shortwave radiation can be measured with the same type of sensor as incoming shortwave, simply mounted in an inverted fashion. See figure 3 for our measurements. Outgoing shortwave can also be modeled. Usually, albedo is the variable modeled and the net shortwave radiation budget is calculated as we saw in equation 1: $SW \downarrow (1 - \alpha)$. A significant amount of effort has gone into measuring albedo using ground- and satellite-based techniques [26]. It is important to get the albedo correct, because a strong feedback exists in the system. For a snow-covered glacier surface, a reduction in albedo increases the amount of radiation absorbed by the surface, which accelerates the snow-ageing processes (impurity content goes up, grain sizes go up, grain shapes change, water content goes up [27]), which reduces the albedo and so on. The albedo of ice surfaces depends on cracks, bubbles, impurities, and whether there is water at the surface, so feedbacks can operate over ice surfaces as well, but they do not tend to be as strong. Calculations of the strength of these feedbacks for Greenland [28] and the Pasterze [29] suggest that the sensitivity of mass balance to changes in temperature goes up by a factor of two. Advanced Very High Resolution Radiometer (AVHRR) and Landsat are the primary satellite datasets that have been used to generate maps of albedo [30] [31] [32] [33] [26]. These images must undergo significant processing before a meaningful map of broadband albedo can be extracted, but they provide a unique and necessary perspective on the albedo for a wide area. Ground measurements range from the simple inverted pyranometer that I mentioned above, to sophisticated instruments that measure the angular and spectral variations in albedo. More than the other terms in the energy-balance, parameterizations of albedo seem to be unique to the glacier for which they were derived. For the Haut Glacier d'Arolla the best relationship for snow albedo (α_s) that Brock *et al.* [34] found for snow deeper than 5 mm water equilavent was

$$\alpha_s = 0.71 - 0.11\, log_{10}(T_{ma}) \tag{22}$$

where T_{ma} is the accumulated amount of daily maximum temperatures above 0 ^{o}C since the last snow fall. Debris content explains the largest portion of the variance observed in ice albedos (α_i). Polar glaciers tend to have low debris content and therefore a relatively high albedo. Some glaciers show an increase of α_i with elevation, other glaciers show no trend. Quoting from Greuell and Genthon [19], "during the melt season α_i may increase with time, as observed by Oerlemans and Knap (1998) on the Morteratschgletscher (Switzerland), decrease with time, as observed by Reijmer *et al.* (1999) on Vatnajökull (Iceland), or remain

constant, as observed by Greuell *et al.* (1997) on the Pasterze, Austria." [35][36][37] These spatial and temporal patterns have not been figured out yet, but it would be reasonable to assume that it has to do with the surface budget of debris and dust. "Oerlemans (1991/92) proposed to make α_i a function of the difference between the elevation and the equilibrium line altitude (ELA) on the assumption that on a decadal timescale the surface budget of debris and dust is tied to the ELA." [38] For shallow snow packs, Oerlemans and Knap [35] proposed

$$\alpha = \alpha_s + (\alpha_i - \alpha_s)e^{-d/d*} \tag{23}$$

where α_s is the snow albedo, α_i is the ice albedo, d is the thickness of the snow pack on top of the ice and $d*$ is a characteristic depth scale found to be 3.2 cm. Smaller effects that aren't considered in these parameterizations are melt water, incidence angle, and cloud amount.

4 LONGWAVE RADIATION

4.1 Incoming longwave radiation

Incoming longwave radiation can be measured with pyrgeometers and modeled using the following equation (found in [19] and [39]).

$$LW\downarrow = [\epsilon_{cs}\,(1 - n_c^a) + \epsilon_{oc}\,n_c^a]\,\sigma\,T_a^4 \tag{24}$$

where ϵ_{cs} is the clear-sky emittance (given below), n_c is the cloud fraction, a is a tuning parameter found to be 4 by Konzelmann *et al.* [39] for the ETH camp in Greenland when using hourly data, ϵ_{oc} is the emmitance of a totally overcast sky (used as another tuning parameter, found to be 0.952 when using hourly data), σ is the Stephan-Boltzmann constant: $\sigma = 5.67 \times 10^{-8} W/m^2\,K^4$, and T_a is the measured air temperature at 2 m in Kelvin.

$$\epsilon_{cs} = 0.23 + c_L\,\left(\frac{e_a}{T_a}\right)^{1/m} \tag{25}$$

where 0.23 is the clear-sky emittance of a completely dry atmosphere as calculated by the Lowtran7 model. c_L and m are tuning parameters (=0.484 and 8 respectively). e_a, again, is the 2 m vapor pressure in Pascals. These tuning parameters would need to be adjusted to apply the model to a different glacier. The parameters depend on, among other things, the specific patterns of clouds at the location.

Figure 4 shows the incoming and outgoing longwave radiation for the three stations that are measuring it on the Taylor Glacier.

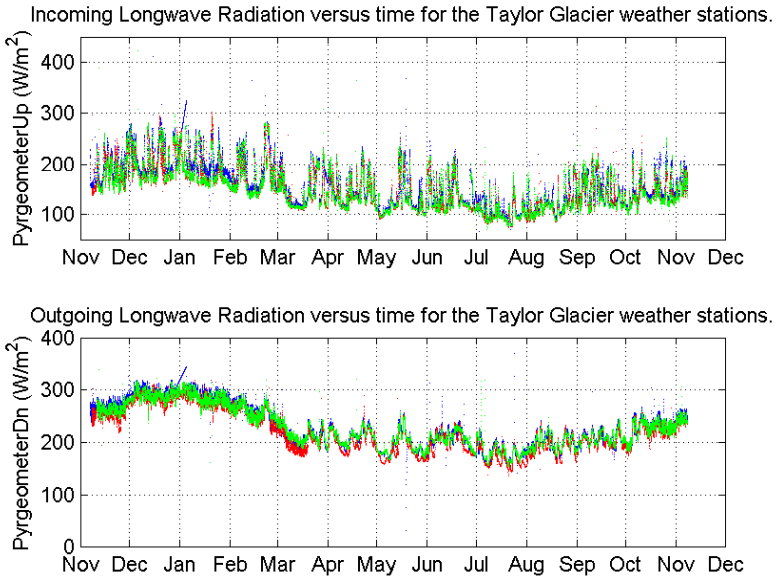

Figure 4: Longwave radiation for the Taylor Glacier. Measured with Kipp and Zonen pyrgeometers.

4.2 Outgoing Longwave Radiation

$$LW \uparrow = \epsilon_s \, \sigma \, T_s^4 + (1 - \epsilon_s) \, LW \downarrow \tag{26}$$

where ϵ_s is the emissivity of the surface snow or ice. T_s is the surface temperature calculated from a subsurface model or assumed to be the melting temperature. The last term on the right hand side of equation 26 is that portion of the incoming longwave radiation that is reflected. Measured and modeled values of ϵ_s are greater than 0.95, indicating that snow and ice are almost perfect black-bodies in the spectral range 4-40 μm. Because of this, ϵ_s is often assumed to be 1 and equation 26 reduces down to

$$LW \uparrow = \sigma \, T_s^4 \tag{27}$$

Greuell and Konzelmann [40] and Greuell and Smeets [41] claim that $LW \uparrow$ calculated using equation 27 with T_s calculated from a multi-layer subsurface temperature model will be more accurate than measurements of $LW \uparrow$.

5 SENSIBLE AND LATENT HEAT FLUX

Eddy-correlation methods are the best way to measure sensible and latent heat fluxes because the technique calculates the fluxes directly from the data. The problem with eddy-correlation set ups is that the instruments are not robust enough to stand up for long periods of time to the harsh environment glaciers present. That said, eddy-correlation is a good way to validate other methods of determining the sensible and latent heat fluxes over glaciers.

A more robust method is the profile method. It uses measurements of the potential temperature (θ), wind speed (u), and specific humidity (q) at two or more levels to calculate the fluxes. Potential temperature is the temperature a parcel of air would have if it was raised or lowered adiabatically to 1000 mb. Specific humidity is the mass of water vapor per mass of air, including water vapor, in a given volume. The theory behind the profile method lies in the Monin-Obukhov similarity theory

$$\tau = \rho_a \, u_*^2 \tag{28}$$

$$u_* = \frac{\kappa \, z}{\phi_m} \, \frac{\partial u}{\partial z} \tag{29}$$

$$Q_H = \rho_a \, C_{pa} \, u_* \, \theta_* \tag{30}$$

$$\theta_* = \frac{\kappa \, z}{\phi_h} \, \frac{\partial \theta}{\partial z} \tag{31}$$

$$Q_L = \rho_a \, L_s \, u_* \, q_* \tag{32}$$

$$q_* = \frac{\kappa \, z}{\phi_h} \, \frac{\partial q}{\partial z} \tag{33}$$

where τ is the momentum flux (or shear stress), ρ_a is the air density, u_*, θ_*, and q_* are the velocity, temperature, and humidity scales. κ is the von Karman constant ($= 0.4$), z is the height above the surface, C_{pa} is the specific heat capacity of the air ($1005 J/(kgK)$), and L_s is the latent heat of sublimation ($2.84 \times 10^6 J/kg$). ϕ_m and ϕ_h are stability functions that account for the higher turbulence that occurs during periods of instability.

$$\phi_m = 1 + \alpha_m \, \frac{z}{L_{ob}} \tag{34}$$

$$\phi_h = Pr + \alpha_h \, \frac{z}{L_{ob}} \tag{35}$$

$$L_{ob} = \frac{u_*^2}{\kappa \, \left(\frac{g}{T_a} \right) \, (\theta_* + 0.62 \, T_a \, q_*)} \tag{36}$$

where α_m, α_h, and Pr (Prandtl number) are empirically derived and as such they vary from study to study and glacier to glacier. For a vegetated area, Högström [42] found α_m = 6.0, α_h = 7.8, and Pr = 0.95. This set of equations 28–36 must be solved iteratively because of the interdependencies within them. Munro [43] goes into more detail. To get the gradients in equations 29, 31, and 33 one must interpolate bewteen measurements at two or more heights above the glacier surface. An alternative if measurements from only two levels exist is the integral form of those equations. Using u_* as an example

$$u_* = \frac{\kappa \left(u_{L2} - u_{L1}\right)}{\ln \frac{z_{L2}}{z_{L1}} + \frac{\alpha_m}{L_{ob}} \left(z_{L2} - z_{L1}\right)} \tag{37}$$

where the subscripts $L1$ and $L2$ represent the two levels of measurements.

If measurements are only available from one level, equations 30 and 32 get integrated from the measurement height down to the surface. This produces the equations for the bulk method of computing the sensible and latent heat fluxes

$$Q_H = \rho_a \, C_{pa} \, \frac{\kappa^2 \, u \left(T_a - T_s\right)}{\left(\ln \frac{z}{z_0} + \frac{\alpha_m \, z}{L_{ob}}\right) \left(\ln \frac{z}{z_T} + \frac{\alpha_h \, z}{L_{ob}}\right)} \tag{38}$$

$$Q_L = \rho_a \, L_s \, \frac{\kappa^2 \, u \left(q_a - q_s\right)}{\left(\ln \frac{z}{z_0} + \frac{\alpha_m \, z}{L_{ob}}\right) \left(\ln \frac{z}{z_q} + \frac{\alpha_h \, z}{L_{ob}}\right)}. \tag{39}$$

T_s comes from a subsurface model or the zero-degree assumption and q_s can be calculated from T_s by

$$q_s = 0.621 \, \frac{e_{sat} \, T_s}{p} \tag{40}$$

where p is atmospheric pressure and e_{sat} is the saturation vapor pressure at T_s.

Temperature measurements for the Taylor Glacier were shown in figure 2. Wind speed is in figure 5 and vapor pressure is in figure 6.

It turns out that the largest uncertainty in these calculation comes from z_o. It can be estimated by extrapolating wind speed data to the point where the speed goes to zero (we are assuming that there is friction between the glacier and the air so that the speed close to the interface must go to zero). The problem when doing this over a rough glacier surface is where to define the reference height (i.e. where do you hold the tape when measuring the instrument heights in relation to the crests and troughs of the small-scale glacier topography). One

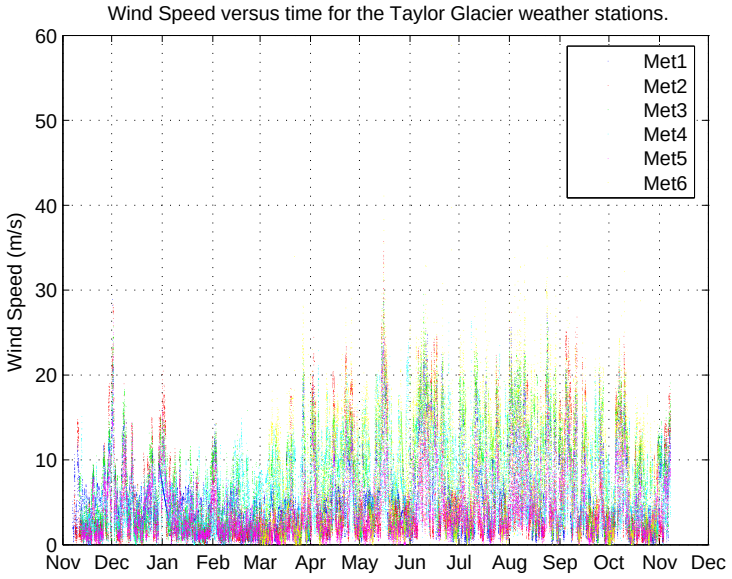

Figure 5: Wind speed for the Taylor Glacier stations. Met6 is recording on a different interval than the rest of the stations, so its data is not directly comparable.

way to get around this problem is to measure the micro-topography of the glacier surface near the station. This is the only available way to get a local z_0 for stations with only one wind sensor. Published values of z_0 range from .1 to 10 mm. Three of the stations on the Taylor Glacier have wind measurements at two-levels, allowing a calculation of z_0. The results of this calculation are in line with what previous investigators have found (figure 7).

The roughness lengths for temperature and moisture can be related to that for momentum by

$$\ln\left(\frac{z_T}{z_0}\right) = 0.317 - 0.565\, R_* - 0.183\, R_*^2 \tag{41}$$

$$\ln\left(\frac{z_q}{z_0}\right) = 0.396 - 0.512\, R_* - 0.180\, R_*^2 \tag{42}$$

$$R_* = \frac{u_*\, z_0}{\nu} \tag{43}$$

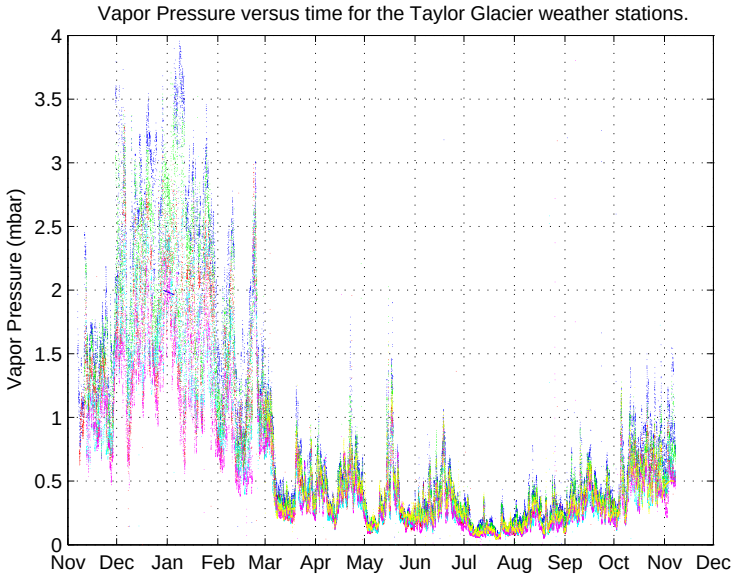

Figure 6: The vapor pressure on the Taylor Glacier is largely controlled by the temperature.

where R_* is the Reynolds number and ν is the kinematic viscosity of air $(1.461 \times 10^{-5} m^2/s)$.

The availability of data dictates which of the methods discussed above would be most appropriate. Box and Steffen [44] give a detailed comparison of eddy-correlation, a profile method, and the bulk method for the Greenland Climate Network stations. Denby and Greuell [45] compare the bulk and profile methods. Munro (e.g. [43]) has done extensive work comparing different techniques.

6 HEAT FLUX DUE TO RAIN

This term is generally negligible, especially for Antarctic glaciers that receive only trace amounts of rain some years and none at all most years. During an event with heavy rain and high temperatures, the term could become important [46]. It can be modeled as

$$Q_R = \rho_w \, r \, C_{pw} \, (T_r - T_s) \tag{44}$$

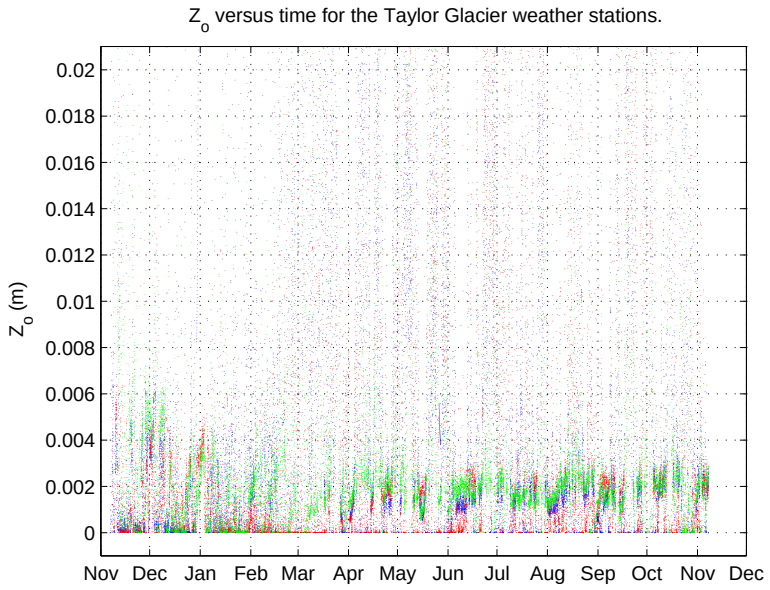

Figure 7: z_0 for the three stations that have wind measurements at two levels. The scale has been truncated at 0.02 meters so that the most common (small) values are visible.

where ρ_w is the water density ($1000kg/m^3$), r is the rainfall rate in m/s, C_{pw} is the specific heat capacity of water, T_r is the rain temperature, and T_s is the surface temperature. For lack of a better measure, T_r can be assumed equal to the measured air temperature at 2 m.

7 SUBSURFACE HEAT FLUX

Heat flux into or out of the glacier can take a number of forms. 1) A small percentage of the incoming solar radiation will be absorbed below the surface of the glacier. 2) If there are temperature gradients within the ice or between the ice and the overlying air, heat conduction will tend to smooth out those gradients. 3) Percolation of meltwater or rain into a sub-freezing snowpack will warm the snowpack as the water freezes and releases its heat of fusion. 4) Air convection in the pore spaces in snow may be significant under high wind or other extreme conditions. A variety of simple parameterizations have been developed for these processes as well as some more complicated models that try

to physically represent what is going on (e.g. [47] [40] [48]) but so far none of them focus on polar glaciers and many of the simple equations assume the surface is at the melting point. The finite-difference temperature model for an iceberg by Bliss and Cuffey (unpublished, 2003) should be applicable to this problem after a few modifications.

8 TECHNIQUES USED TO DISTRIBUTE WEATHER VARIABLES

- Linear interpolation between locations of measurements (many studies).
- Interpolation using splines or other functions.
- Linear regression of the meteorological observations with elevation (apply a constant lapse rate) or with distance from the watershed divide (again, many refs).
- Some authors (e.g. [5]) also make a correction to the lapse rate model that uses the residuals from the linear model. These residuals are spatially interpolated by applying an inverse distance weighting approach. At the station, the calculated value will equal the station measurement; away from the station, the linear model is modified by adding a term like $\frac{residual}{distancefromstation}$.

Figure 8 shows an example of this type of interpolation. All of these interpolation schemes work best for temperature, because temperature typically follows a fairly regular lapse rate. However, parameters like relative humidity and wind speed do not typically follow a regular lapse rate, so additional interpolation techniques are needed. It is more appropriate to use specific humidity than relative humidity, because specific humidity does not depend on temperature.

9 FUTURE IMPROVEMENTS TO ENERGY-BALANCE MODELS

To improve the accuracy of energy-balance models' response to climate change, one should add a parameterization relating the free-atmosphere and near-surface variables. Global climate models can help with this - they provide the free-atmosphere variables and the task is then to write a relationship that can predict ablation for the present day given the

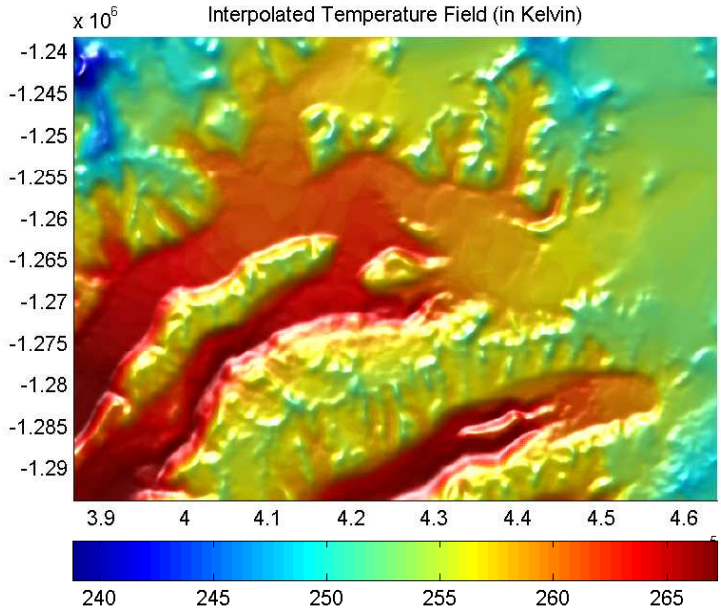

Figure 8: Temperature in the vicinity of the Taylor Glacier on November 13th, 2003 at 00:00. This field is calculated from the weather station data as the sum of an elevation-dependent field and a field that spatially interpolates the measured deviations from the elevation-dependent field.

free-atmosphere conditions. The free-atmosphere variables are the ones that will be predicted by climate-change scenario models. One would have to make some assumptions or additional parameterizations to say how the relation between the free-atmosphere and near-surface characteristics changed with the climate. Energy-balance models have no capacity for predicting precipitation, for example, so the other types of models discussed in the beginning of this paper would need to take up the slack to get a clear picture of the future mass balance of glaciers around the world.

Author Affiliation:

Andrew Bliss
Department of Geography
University of California at Berkeley
507 McCone Hall
Berkeley, CA 94720-4740 USA
Tel: 510.642.3946

References

[1] K. M. Cuffey, G. D. Clow, R. B. Alley, M. Stuiver, E. D. Waddington, and R. W. Saltus. Large arctic temperature-change at the wisconsin-holocene glacial transition. *Science*, 270(5235):455 – 458, 1995.

[2] R. Hock and H. Jensen. Application of kriging interpolation for glacier mass balance computations. *Geografiska Annaler Series A-Physical Geography*, 81A(4):611 – 619, 1999.

[3] R. J. Braithwaite. Positive degree-day factors for ablation on the greenland ice-sheet studied by energy-balance modeling. *Journal of Glaciology*, 41(137):153 – 160, 1995.

[4] R. J. Braithwaite and Y. Zhang. Sensitivity of mass balance of five swiss glaciers to temperature changes assessed by tuning a degree-day model. *Journal of Glaciology*, 46(152):7 – 14, 2000.

[5] U. Strasser, J. Corripio, F. Pellicciotti, P. Burlando, B. Brock, and M. Funk. Spatial and temporal variability of meteorological variables at haut glacier d'arolla (switzerland) during the ablation season 2001: Measurements and simulations. *Journal of Geophysical Research-Atmospheres*, 109(D3), 2004.

[6] B. W. Brock and N. S. Arnold. A spreadsheet-based (microsoft excel) point surface energy balance model for glacier and snow melt studies. *Earth Surface Processes and Landforms*, 25(6):649 – 658, 2000.

[7] C. H. Reijmer and J. Oerlemans. Temporal and spatial variability of the surface energy balance in dronning maud land, east antarctica. *Journal of Geophysical Research-Atmospheres*, 107(D24), 2002.

[8] E. J. Klok and J. Oerlemans. Model study of the spatial distribution of the energy and mass balance of morteratschgletscher, switzerland. *Journal of Glaciology*, 48(163):505 – 518, 2002.

[9] K. J. Lewis, A. G. Fountain, and G. L. Dana. Surface energy balance and meltwater production for a dry valley glacier, taylor valley, antarctica. *Annals of Glaciology*, 27:603 – 609, 1998.

[10] G. D. Clow, C. P. McKay, G. M. Simmons, and R. A. Wharton. Climatological observations and predicted sublimation rates at lake hoare, antarctica. *Journal of Climate*, 1(7):715–728, 1988.

[11] R. J. Braithwaite and O. B. Olesen. A simple energy-balance model to calculate ice ablation at the margin of the greenland ice-sheet. *Journal of Glaciology*, 36(123):222 – 228, 1990.

[12] H. Gallée. Mesoscale atmospheric circulations over the southwestern ross sea sector, antarctica. *Journal of Applied Meteorology*, 35(7):1129 – 1141, 1996.

[13] C. Genthon and A. Braun. Ecmwf analyses and predictions of the surface climate of greenland and antarctica. *Journal of Climate*, 8(10):2324 – 2332, 1995.

[14] R. W. Glover. Influence of spatial resolution and treatment of orography on gcm estimates of the surface mass balance of the greenland ice sheet. *Journal of Climate*, 12(2):551 – 563, 1999.

[15] D. H. Bromwich, A. J. Monaghan, J. G. Powers, J. J. Cassano, H. L. Wei, Y. H. Kuo, and A. Pellegrini. Antarctic mesoscale prediction system (amps): A case study from the 2000-01 field season. *Monthly Weather Review*, 131(2):412 – 434, 2003.

[16] G. Krinner and C. Genthon. Gcm simulations of the last glacial maximum surface climate of greenland and antarctica. *Climate Dynamics*, 14(10):741 – 758, 1998.

[17] G. Krinner, C. Genthon, Z. X. Li, and P. Levan. Studies of the antarctic climate with a stretched-grid general circulation model. *Journal of Geophysical Research-Atmospheres*, 102(D12):13731 – 13745, 1997.

[18] M. Wild and A. Ohmura. Change in mass balance of polar ice sheets and sea level from high-resolution gcm simulations of greenhouse warming. *Annals of Glaciology*, 30:197 – 203, 2000.

[19] W. Greuell and C. Genthon. Modelling land-ice surface mass balance. In J. L. Bamber and A. J. Payne, editors, *Mass Balance of the Cryosphere*, chapter 5, pages 117–168. Cambridge University Press, Cambridge, UK, 2004.

[20] F. Kasten. A new table and approximation formula for the relative. *Arch. Meteorol. Geophys. Bioklimatol. Ser. B*, 14:206–223, 1966.

[21] A. J. Prata. A new long-wave formula for estimating downward clear-sky radiation at the surface. *Quarterly Journal of the Royal Meteorological Society*, 122(533):1127 – 1151, 1996.

[22] R. Bintanja and M. R. Van den Broeke. The influence of clouds on the radiation budget of ice and snow surfaces in antarctica and greenland in summer. *International Journal of Climatology*, 16(11):1281 – 1296, 1996.

[23] N. Robinson. *Solar Radiation*. Elsevier Pub. Co., Amsterdam, 1966.

[24] M. Iqbal. *An Introduction to Solar Radiation*. Academic Press, Toronto, Canada, 1983.

[25] J. G. Corripio. Vectorial algebra algorithms for calculating terrain parameters from dems and solar radiation modelling in mountainous terrain. *International Journal of Geographical Information Science*, 17(1):1 – 23, 2003.

[26] W. H. Knap, B. W. Brock, J. Oerlemans, and I. C. Willis. Comparison of landsat tm-derived and ground-based albedos of haut glacier d'arolla, switzerland. *International Journal of Remote Sensing*, 20(17):3293 – 3310, 1999.

[27] S. G. Warren. Optical properties of snow. *Reviews of Geophysics*, 20(1):67 – 89, 1982.

[28] R.S.W. Van de Wal. Mass-balance modelling of the greenland ice sheet: a comparison of energy-balance and a degree-day model. *Annals of Glaciology*, 23:36–45, 1996.

[29] W. Greuell and R. Böhm. 2 m temperatures along melting mid-latitude glaciers, and implications for the sensitivity of the mass balance to variations in temperature. *Journal of Glaciology*, 44(146):9 – 20, 1998.

[30] E. J. Klok and J. Oerlemans. Modelled climate sensitivity of the mass balance of morteratschgletscher and its dependence on albedo parameterization. *International Journal of Climatology*, 24(2):231 – 245, 2004.

[31] E. J. Klok, W. Greuell, and J. Oerlemans. Temporal and spatial variation of the surface albedo of morteratschgletscher, switzerland, as derived from 12 landsat images. *Journal of Glaciology*, 49(167):491 – 502, 2003.

[32] M. S. D. De wildt, J. Oerlemans, and H. Bjornsson. A method for monitoring glacier mass balance using satellite albedo measurements: application to vatnajokull, iceland. *Journal of Glaciology*, 48(161):267 – 278, 2002.

[33] W. H. Knap, C. H. Reijmer, and J. Oerlemans. Narrowband to broadband conversion of landsat tm glacier albedos. *International Journal of Remote Sensing*, 20(10):2091 – 2110, 1999.

[34] B. W. Brock, I. C. Willis, M. J. Sharp, and N. S. Arnold. Modelling seasonal and spatial variations in the surface energy balance of haut glacier d'arolla, switzerland. *Annals of Glaciology*, 31:53 – 62, 2000.

[35] J. Oerlemans and W. H. Knap. A 1 year record of global radiation and albedo in the ablation zone of morteratschgletscher, switzerland. *Journal of Glaciology*, 44(147):231 – 238, 1998.

[36] C. H. Reijmer, W. H. Knap, and J. Oerlemans. The surface albedo of the vatnajokull ice cap, iceland: A comparison between satellite-derived and ground-based measurements. *Boundary-Layer Meteorology*, 92(1):125 – 144, 1999.

[37] W. Greuell, W. H. Knap, and P. C. Smeets. Elevational changes in meteorological variables along a midlatitude glacier during summer. *Journal of Geophysical Research-Atmospheres*, 102(D22):25941 – 25954, 1997.

[38] J. Oerlemans. A model for the surface balance of ice masses: part i. alpine glaciers. *Z. Gletscherkd. Glazialgeol.*, 27/28:63–83, 1991/2.

[39] T. Konzelmann, R. S. W. Vandewal, W. Greuell, R. Bintanja, E. A. C. Henneken, and A. Abeouchi. Parameterization of global and longwave incoming radiation for the greenland ice-sheet. *Global and Planetary Change*, 9(1-2):143 – 164, 1994.

[40] W. Greuell and T. Konzelmann. Numerical modeling of the energy-balance and the englacial temperature of the greenland ice-sheet - calculations for the eth-camp location (west greenland, 1155m asl). *Global and Planetary Change*, 9(1-2):91 – 114, 1994.

[41] W. Greuell and P. Smeets. Variations with elevation in the surface energy balance on the pasterze (austria). *Journal of Geophysical Research-Atmospheres*, 106(D23):31717 – 31727, 2001.

[42] U. Högström. Non-dimensional wind and temperature profiles in the atmospheric surface-layer - a re-evaluation. *Boundary-Layer Meteorology*, 42(1-2):55 – 78, 1988.

[43] D. S. Munro. Surface-roughness and bulk heat-transfer on a glacier - comparison with eddy-correlation. *Journal of Glaciology*, 35(121):343 – 348, 1989.

[44] J. E. Box and K. Steffen. Sublimation on the greenland ice sheet from automated weather station observations. *Journal of Geophysical Research-Atmospheres*, 106(D24):33965 – 33981, 2001.

[45] B. Denby and W. Greuell. The use of bulk and profile methods for determining surface heat fluxes in the presence of glacier winds. *Journal of Glaciology*, 46(154):445 – 452, 2000.

[46] J. E. Hay and B. B. Fitzharris. A comparison of the energy-balance and bulk-aerodynamic approaches for estimating glacier melt. *Journal of Glaciology*, 34(117):145 – 153, 1988.

[47] E. Brun, P. David, M. Sudul, and G. Brunot. A numerical-model to simulate snow-cover stratigraphy for operational avalanche forecasting. *Journal of Glaciology*, 38(128):13 – 22, 1992.

[48] M. Lehning, P. Bartelt, B. Brown, T. Russi, U. Stockli, and M. Zimmerli. Snowpack model calculations for avalanche warning based upon a new network of weather and snow stations. *Cold Regions Science and Technology*, 30(1-3):145 – 157, 1999.